Desalination and Water Treatment
www.deswater.com

doi:10.5004/dwt.2017.0687

69 (2017) 18–28
March

Influence of amine functionalization of silica particles fillers on the morphology and water permeation of polyethersulfone nanocomposite ultrafiltration membranes

Antonio Martín[a], Jesús M. Arsuaga[a], Nuria Roldán[a], Ana Martínez[b], Arcadio Sotto[a,*]

[a]*School of Experimental Science and Technology, ESCET, Rey Juan Carlos University, Spain, emails: antonio.martin.rengel@urjc.es (A. Martín), arcadio.sotto@urjc.es (A. Sotto)*
[b]*Department of Applied Mathematics, Technical University of Madrid, Spain, emails: jesusmaria.arsuaga@urjc.es (J.M. Arsuaga), n.roldancas@gmail.com (N. Roldán), ana.martinez@upm.es (A. Martínez)*

Received 20 June 2016; Accepted 14 July 2016

ABSTRACT

A wide characterization of morphological features of mesoporous silica doped polyethersulfone ultrafiltration membranes is accomplished in this investigation. Different amine-functionalization routes of pure SBA-15 were carried out to obtain a variety of materials with specific physico-chemical properties. The effect of amine-functionalization on the textural and morphological characteristics of particles was analyzed by nitrogen physisorption, transmission electronic microscopy (TEM), and dynamic light scattering (DLS). The incorporation yield of amino groups to the SBA-15 structure was corroborated by elemental analysis (HCNS). The morphology of membrane was investigated by scanning electronic microscopy (SEM) and field emission gun-scanning (FEG-SEM) to analyze the cross-section and surface characteristics. The addition of a small amount of functionalized silica particles enhanced the interconnectivity of the pores and membrane hydrophilicity. Water permeation experiments in cross-flow configuration were carried out to clarify the effect of membranes physico-chemical properties on the filtration performance. The selected concentration for fillers ranged from 0.3 wt.% to 2.0 wt.% and best results were found for 0.6 wt.% according to the observed permeation potential of prepared membranes. The relation between water permeation and membrane surface properties was analyzed in terms of pore size, porosity, and hydrophilicity. The influence of pore circularity on water flux was also explored, suggesting the importance of this parameter in the rigorous analysis of membrane porosity. The study of the thermodynamic stability of the quaternary system involved in the membrane formation (polymer, solvent, non solvent, filler) corroborated the influence of the fillers incorporation on the membrane morphology.

Keywords: Polyethersulfone; Ultrafiltration doped membrane; Amine-functionalized SBA-15; Surface porosity; Membrane formation thermodynamics

1. Introduction

Nanocomposite membranes are a new category of membranes that have recently appeared for a wide range of purposes in the membrane technologies [1,2]. In general, they can be described as a discontinuous phase on nanoscale embedded in a continuous phase or matrix. For example, metals, metal oxides, molecular sieves, and so on, are incorporated as nanofillers, fully surrounded by a continuous matrix that is often an organic polymer.

Many authors report the advantages of the addition of nanofillers on the membrane properties: suppression

*Corresponding author.

Presented at the EDS conference on Desalination for the Environment: Clean Water and Energy, Rome, Italy, 22–26 May 2016

of macrovoids, improved mechanical strength and lifetime, enhanced interconnectivity of the pores resulting in a superior permeability combined with unchanged retention properties [3–6]. Superior antifouling properties of doped membranes are also an important goal that explain the wide investigation performed in this field in the last years [7,8].

It is expected that the added nanoparticles might provide a direct pathway for water transport or modify the membrane network structure, thereby increasing water permeability [9,10]. The addition of a hydrophilic substance in the casting solution leads to an acceleration of solvent and non-solvent exchange and is advantageous to form the porous structure. The increase in the membrane porosity enhances the permeability. The improved hydrophilicity due to the intrinsic hydrophilic character of the entrapped nanofillers strengthens the attraction of water molecules to the inner structure of the membrane matrix so enhancing the membrane permeability. Therefore, the potential of nanocomposite membranes depends on the selection of a suitable polymer and inorganic nanoparticles based on their properties. However, the nanoparticle type selection is an issue that is not well explained in the literature. Despite this innovative strategy has drawn much attention, the influence of physico-chemical properties of nanofillers type on the membrane performance is an unsolved question.

Another important variable determining the doped membrane performance is the particle size. In the literature is described that a nanoscaled distribution of fillers into the polymer matrix is required to optimize the intercomponent interactions and, therefore, improve membrane functional properties [1]. However, nanoparticles readily aggregate when mixed with an aprotic solvent forming clusters that are within the microscale range. In the last years, some authors have proposed that the addition of a small amount of fillers would result in a high free surface available for the adsorption of the polymer chains. Added particles would yield more polymer/particle interfacial area and provide a chance to disrupt polymer chain packing in different forms. Conversely, high contents of particles decrease water permeation by accumulation onto the membrane surface and pore blocking [11–13]. Thus, it is evident that the amount of incorporated filler should be optimized according to the membrane performance. Some authors recommend particle concentration lower than 2 wt.% [14–16]. The aggregation of particles leads to precipitation of fillers at the bottom of the membrane during the phase inversion, reducing the expected improved effects.

In the second hand, it is crucial to consider the effect of nanoparticle on the membrane morphology. Usually, membrane porosity is calculated by the wet-dry weight method as a measure of membrane free volume. Taking into account the differences in morphology between upper and bottom sides of membranes prepared by phase inversion process, the calculated porosity does not distinguish the individual contribution of both sides. The membrane porosity could be estimated by the wet-dry weight method only if the connectivity between both sides is large enough. In addition, the porosity of non-woven polyester tissue used as mechanical support overloads in many times the porosity of any prepared ultrafiltration membrane. Therefore, the morphological characteristic of skin layer, that is the main responsible of the membrane filtration performance in ultrafiltration (UF), should be studied in terms of surface porosity and pore size distribution.

The pore size distribution of UF membranes is usually calculated by permeation tests, determining a "functional pore". Thus, some authors using the classical Guerout–Elford–Ferry equation for pure water permeation [17] or by filtration of uncharged compounds through nanofiltration and ultrafiltration membranes determine the mean pore diameter of membranes using an algorithm that incorporates the pore flow model [18]. This last model assumes that the permeation of neutral solutes in pores is governed by steric hindrance mechanisms. These models are very useful to predict the membrane performance for specific applications [19] in the water treatment.

Alternatively, pore size distribution can be obtained by direct determination of "physical pore" using electronic microscopy (FEG-SEM). The study of pore size distribution by direct methods gives true information about the physical dimensions of pores that leads to estimate the membrane porosity by the following equation:

$$\text{Surface porosity}\,(\%) = \frac{\sum_i n_i S_i}{\sum_i S_i} = \frac{\sum_i n_i S_i}{S_T} \quad (1)$$

where S_i refers to specific pore areas and n_i to the corresponding number. Using Eq. (1) it is possible to obtain accurate information about the area occupied by the membrane surface pores. Another interesting issue could be the presence of "blind pores" on the membrane surface not connected with the inner structure of membrane, specifically with the macrovoids formed in the subsequent layer. The connectivity of membrane morphology can be explored by SEM cross-section analysis [20].

Some authors affirm that the incorporation of hydrophilic particles leads to hydrophilicity increase of polymeric membranes but does not affect the pore size or pores number of modified membranes [21]. Other authors, to the contrary, consider that the nanofillers can act as pore forming agents [22]. Concerning this effect, a very interesting question appears: Is it possible to find a numerical correlation between the number of doping particles and the number of formed pores? Probably not, because the pore formation in these modified membranes is a complex process determined by the thermodynamics and kinetics of a quaternary system during the membrane formation. Unfortunately, it is a matter understudied.

It is also important to explore the effect of particle incorporation into the polymeric solution before membrane formation [23–25]. The polymer chains distribution is modified around the zones occupied by the added particles. Thus, the polymeric chains disturbance should depend on the size, shape and surface activity of incorporated filler. It is expected that near added filler, large pores could be generated during the membrane formation. Thus, particle incorporation increases the pore size range in comparison with neat membrane while modifies the geometry and shape of new promoted pores. Therefore, the geometry (circularity) of pore mouth is analyzed in this study.

Thermodynamic and kinetic studies of the precipitation process are crucial in the understanding of membrane formation. Thermodynamics of equilibrium composition is

commonly studied with ternary phase diagrams of polymer solution [26,27]. The addition of hydrophilic particles could shifts the bimodal curve toward different nonsolvent concentrations altering the pore formation and the thickness of membrane skin layer [28]. In this investigation, thermodynamics of membrane formation is studied varying the activity surface of particles used as fillers. On the other hand, the viscosity of the casting solution negatively affects the solvent/nonsolvent exchanging rate during phase inversion process [29]. High viscous polymeric solutions restrict the interdiffusion during this process delaying the membrane formation and, hence, yield a poor surface porosity. This effect is particularly pronounced for polymeric solution with high contents of added particles. Commonly, the observed reduction of flux for membranes prepared at filler concentration higher than 2 wt.% is explained in terms of surface pore blocking and the effect of the skin layer thickness is underestimated.

A very common strategy for increasing the permeation rate is to improve the hydrophilic character of the membrane surface. Thus, many studies have been focused on addition of intrinsically hydrophilic fillers to the polymer matrix looking for the formation of abundant hydrophilic sites both in the surface and inner regions of the doped membrane. Contact angle measurements are often used to evaluate the hydrophilic character of membrane surface. However, contact angle results also depends on the number and size of surface pores that affect the adhesive forces between water molecules and the membrane surface. Hence, it is not clear that a direct correlation could be established between the added hydrophilic particles amount and the permeation performance of the membrane. Therefore, this issue must be considered with some detail.

In this investigation, we have studied the morphology and pure water permeation of ultrafiltration polyethersulfone membranes doped with amine-functionalized mesostructured silica particles. Mesoporous SBA-15 silica was selected as support due to its physical and chemical stability, very high surface area, large pore, narrow pore size distribution, and easy surface functionalization [30]. Four different amine functionalities were incorporated to pure silica particles in order to obtain a variety of hydrophilic fillers with different amino groups content. Since several strategies of functionality incorporation have been proposed in literature [31], two functionalization methods have been selected in this work: hyperbranching polymerization with aziridine and co-condensation from three different amine precursors. The aim of this investigation is to determine how the physicochemical properties of added particles affect the morphology and permeation of doped membranes. Additionally, this work includes a discussion about the ability of different morphological variables commonly used to predict the membrane permeation.

2. Experimental

2.1. Synthesis and characterization of functionalized SBA-15 materials

Three functionalized SBA-15 materials were synthesized by co-condensation method, similar to that of the conventional SBA-15 [30] except for adding a certain amount of selected organosilane 1 h after adding the silica source

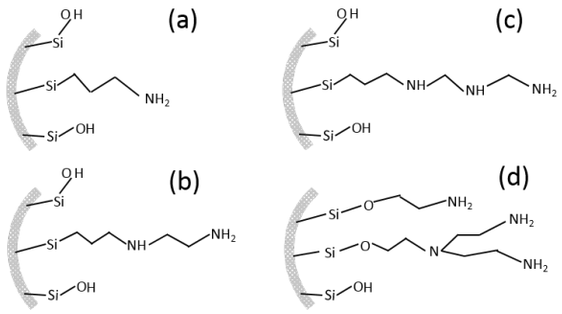

Fig. 1. Material schemes for amine-functionalized SBA-15 particles. (a) SBA-15/monoamine; (b) SBA-15/diamine; (c) SBA-15/triamine; (d) SBA-15/ polyethyleneimine.

(TEOS). In addition, surfactant was removed by ethanol-washing reflux instead of calcination. The organosilanes used as functionalizing agents were 3-(aminopropyl) trimethoxysilane (SBA15/Monoamine), *N*-(3-trimethoxysilylpropyl) ethylenediamine (SBA-15/Diamine), and *N*-(3-trimethoxysilylpropyl)diethylenetriamine (SBA-15/Triamine) (Figs. 1(a)–(c)). SBA-15 functionalized with polyethyleneimine groups was synthesized by hyperbranching polymerization procedure [32]. In this process, the surface polymerization of aziridine was performed with toluene as solvent, in which the SBA-15 substrate was suspended in the presence of catalytic amount of acetic acid. The suspension was refluxed under an argon atmosphere overnight at 348 K, filtered, washed with toluene and dried in vacuo at 313 K (SBA-15/Polyethyleneimine) (Fig. 1(d)).

Structural characterization of fillers was evaluated by transmission electron microscopy (TEM) on a PHILIPS TECNAI-20 electronic microscope operating at 200 kV. Textural properties of the functionalized silica composites were calculated by means of nitrogen adsorption and desorption isotherms at 77 K using a Micromeritics TRISTAR 3,000 equipment. Nitrogen content was determined by means of elemental analysis (HCNS) in a Vario EL III apparatus. Particle size distribution was defined by using a master sizer laser diffraction particle size analyzer (Malvern Instrument Ltd., Malvern, England). Selected particles were dispersed in *N*-methyl-2-pyrrolidone (NMP) or water and sonicated for 15 min using a bath sonicator before the measurements (40 W, 50 Hz, Fisher Scientific Fair Lawn, New Jersey). At least four measurements were carried out in order to verify the repeatability of all hydrodynamic sizes.

2.2. Membrane preparation

Membranes were prepared by phase inversion induced by immersion-precipitation method. The casting solution was prepared using polyethersulfone (PES, 58 kDa) provided by Solvay Chemicals International (Belgium), and *N*-Methyl-2-Pyrrolidone (NMP) supplied by Scharlau (Barcelona, Spain) used as polymer solvent. Polymer concentration was fixed at 16 wt.%. Table 1 summarizes the particle concentration of casting solutions used in this study and the nomenclature proposed to differentiate the tested membranes.

2.3. Membrane characterization

Cross-section structure of membranes was analyzed using a Scanning Electron Microscopy (SEM, XL-30, Philips, Eindhoven, The Netherlands). The membrane surface was imaged by using a Field Emission Gun Scanning Electron Microscope (FEG-SEM, FEI Co.) and the micrographs were analyzed in order to calculate the membrane surface porosity and pore size distributions. The statistical membrane surface porosity was estimated from the averaged values obtained from four samples of each membrane type.

Fig. 2 shows the surface image of membrane and the corresponding statistical analysis of pore size distribution. In addition to surface porosity (Eq. 1), the surface pores density was analyzed as follows in Eq. (2):

$$\text{Surface pores density} = \frac{\text{Pores number}}{\text{Surface area}} \quad (2)$$

Overall porosity of membranes was calculated through water uptake as a function of the membrane weight. Membrane samples were immersed in water during 24 h to ensure saturation prior to the swelling state measurement. The water content was determined from the weight difference before and after hydration of the membrane to evaluate the overall membrane porosity with Eq. (3):

$$\text{Overall porosity}(\%) = \left(\frac{W_w - W_d}{S d \rho}\right) \cdot 100 \quad (3)$$

where W_w and W_d are the equilibrium weights of a membrane at swelling and dry states, respectively; S is the membrane area; d is the thickness, and ρ is the density of water. Four samples of each type of doped membranes were analyzed to obtain the porosity data.

The thermodynamic ternary phase diagram (polymer, solvent, and water) was constructed by determining the cloud point of the casting solutions (16 wt.% PES and 84 wt.% solvent) by the titration method. The casting solution was introduced in a shield vessel and was constantly stirred at room temperature. The non-solvent solution (60 wt.% of solvent and 40 wt.% of distilled water) was added drop by drop using a syringe until constant turbidity on the solution was achieved. The phase separation kinetics of membrane formation process was studied by measuring the viscosity of the casting solution. For this purpose, a rotational rheometer (Brookfield) was used at constant temperature (25°C) and angular velocity between 5 and 200 rpm.

Surface hydrophobicity/hydrophilicity of the polymeric membranes were determined by contact angle values of a water drop deposited on the membrane surface using a KSV CAM 200 instrument (KSV Instruments, USA).

Table 1
Membranes prepared in this investigation

Membrane	Nomenclature	Filler content (wt.%)
PES	Neat	0.6
PES/SBA-15/Monoamine	Monoamine	0.6
PES/SBA-15/Diamine	Diamine	0.6
PES/SBA-15/Triamine 0.6	Triamine	0.6
PES/SBA-15/ Polyethyleneimine	Polyamine	0.6
PES/SBA-15/Triamine 0.3	Triamine 0.3	0.3
PES/SBA-15/Triamine 1.0	Triamine 1.0	1.0
PES/SBA-15/Triamine 2.0	Triamine 2.0	2.0

2.4. Filtration experiments

Filtration experiments were carried out by using a Teflon cross-flow cell module with an effective membrane area of 0.0015 m^2 connected to a 2 L volume tank. Membrane samples were previously compacted at 3 bar with distilled water for 2 h before the measurements. The membrane permeability for pure water was determined in a filtration recycle mode under 2 bar of pressure and a feed temperature of 25°C.

Additional experiments were performed to determine the molecular weight cut-off (MWCO) of membranes

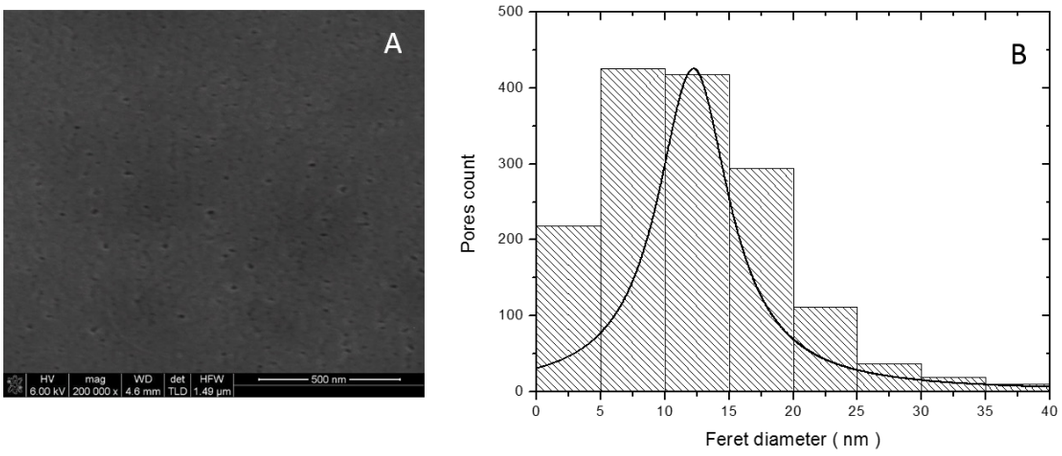

Fig. 2. (A) FEG-SEM image of Triamine modified membrane; (B) Pore size distribution of Triamine modified membrane.

through filtration tests of aqueous solutions containing a mixture of polyethylene glycols (PEOs) of different molecular weights.

3. Results

3.1. Characterization of amine functionalized SBA-15 particles

The internal ordered arrangement of functionalized SBA-15-type particles has been confirmed by transmission electronic microscopy (TEM). TEM images of (A) SBA-15/Monoamine, (B) SBA-15/Diamine, (C) SBA-15/ Triamine, and (D) SBA-15/ Polyethyleneimine are shown in Fig. 3. These images evidence successive clear and dark areas corresponding to the empty pores and pore walls of the well defined mesoporous channels typical of this type of structured materials [30]. Moreover, it must be noted that polymeric aggregates were not observed, supporting the hypothesis of a homogeneous distribution of the organic functionalization throughout the mesoporous framework.

The textural properties of different amine-modified mesoporous materials as well as purely siliceous mesostructured SBA-15 were determined by nitrogen sorption at 77 K. The organically-modified samples exhibit adequate textural parameters, lower than those of pure SBA-15 (S_{BET}, 620 m^2g^{-1}), but still well within the mesoporous range as shown inside Fig. 4. This fact suggests a successful incorporation of the organic functionality. Fig. 4 also displays the amount of amino groups per unit of BET surface area as function of nitrogen content for the different synthesized materials.

In the case of the samples synthesized by co-condensation method, the amino groups concentration is approximately proportional to the nitrogen content. However, the sample modified with polyethyleneimine by hyperbranching presents a very higher ratio as consequence of nitrogen content increment and simultaneous BET surface reduction. Perhaps, the decrease of accessible BET area is due to the organic moieties aggregation near the entries of the mesoporous channels and the outer surface of the SBA-15 particles.

Particle size of fillers dispersed in different solvents and its effect on the membrane water permeation is discussed below in section 3.4.

3.2. Morphological characterization of membranes

The membrane morphology is usually studied in terms of macrovoids configuration as result of kinetics of solvent-nonsolvent interdiffusion process during the membrane formation [33,34]. This issue is explored by using SEM technique taking cross-section images of prepared membranes. As seen in Fig. 5, all membranes exhibit similar asymmetric patterns with large inner macrovoids in their structure. However, some differences are appreciable comparing the upper layer of membranes and the connectivity between membrane skin and inner macrovoids.

As result of comparison of Figs. 5(A) and (C) is possible to conclude that the 1.0 wt.% addition of filler content to the membrane composition promotes a thicker upper layer and the formation a sponge like-structure in the morphology of

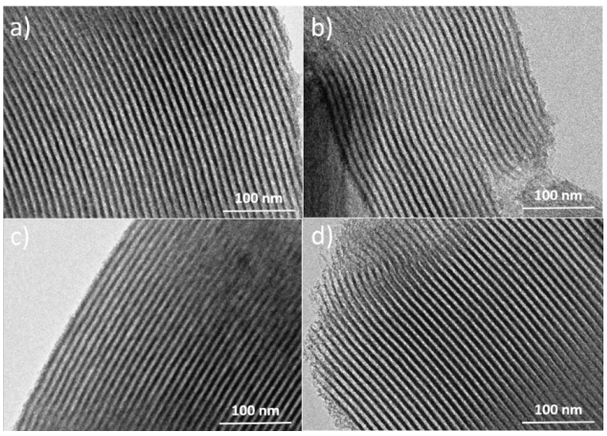

Fig. 3. TEM images of synthesized materials. (a) SBA-15/monoamine; (b) SBA-15/diamine; (c) SBA-15/triamine; (d) SBA-15/polyethyleneimine.

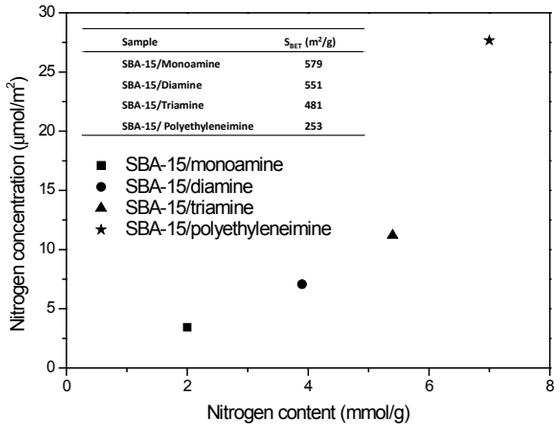

Fig. 4. Amount of amino groups per unit of BET surface area vs. nitrogen content for the different synthesized materials.

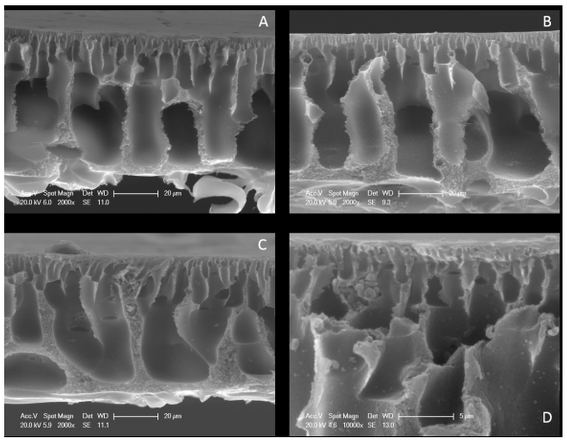

Fig. 5. Cross section images of prepared membranes. (A) Neat; (B) Triamine; (C) Triamine 1.0 (magnification 2, 000X); (D) Triamine 1.0 (magnification 10, 000X).

membrane inner structure. These facts can be explained in terms of solution viscosity increase due to the addition of solid particles to the polymeric solution that restricts the kinetics of membrane formation process [26]. At lower filler concentration (Fig. 5(B)) the connectivity between upper and bottom sides of membrane is improved with direct channels connecting the surface and inner porous of membranes. Taking into account that the thickness of skin layer plays an important role in the permeation potential of membrane as a flux resistance factor, is crucial to control the skin layer rise.

3.3. Water permeation experiments

Fig. 6 shows the observed values of water flux as function of both particle concentration and modification type.

Following the objective proposed in this study, it is important, first at all, to explore the influence of particle modification type on the membrane filtration (Fig. 6(A). For the same particle synthesis route, namely co-condensation, the membrane water permeation increases as rises the amino groups incorporated to particles surface. Conversely, in the case of hyperbranching synthesis procedure, the flux value drops, being similar to Monoamine membrane. It seems that the functionalization extent is important, but not sufficient to guarantee a better filtration performance. The length chain effect of incorporated amine functionality modifies the interaction grade between polymer and fillers. As result of this study, we have selected SBA-15/Triamine as model filler to investigate the influence of doping particle concentration in the casting solution on the water permeate flux (Fig. 6(B). An apparent maximum is observed for water flux at 0.6 wt.% concentration of particles. For values higher than 1 wt.%, the membrane permeation does not improve in comparison with neat membrane, rather declines. Some authors, in the case of TiO_2 fillers, explain this behavior in terms of pore blocking as result of agglomeration of particles onto the membrane surface [12]. The image shown in Fig. 5(D) clearly shows the presence of agglomerates formed near the membrane surface. In addition, the increased viscosity of the casting solution with higher particle content could promote the formation of thicker skin layer. Both effects would be responsible of the mechanical restriction of water transport that explains the performance of membrane filtration as function of doping particle concentration.

3.4. Effect of particle size

The incorporation of fillers to the casting polymer composition affects the membrane formation. In this sense, the influence of particle size should be explored. Different approaches have been proposed to decrease the aggregation degree as a promising way to achieve the highest interaction between polymer and fillers [33]. Chemical and mechanical treatments have been applied to improve the dispersion of particles in the polymeric solution [13,15,35]. The adsorption of polymer chains onto the surface of particles alters their possible configurations. Therefore, the type of functional group incorporated to filler surface will be crucial in the conformational energy of this ternary system (polymer, solvent and filler). In addition, particle aggregation could also modify the interaction strength between filler and polymer chains as result of reduction of accessible adsorption sites.

The effect of particle size has been studied for fillers dispersed in two different media: the polymer solvent used in this investigation, NMP, and water. Fig. 7 shows the mean size values as function of particle modification. Experimental mean sizes measured in water are quite similar for all amine-functionalized materials and larger than neat SBA-15 value (Fig. 7(A)). Moreover, the obtained sizes are alike to values estimated from TEM so evidencing that particle aggregation is not significant in water. The good dispersion could be associated to electrostatic repulsion between particles as result of formation of double electric layer around the particle surface. Conversely, experimental values in NMP solvent exhibit significant differences in particle size (Fig. 7(B)). The enhancement of amino groups on the surface of functionalized particles promotes the formation of particles aggregates in this aprotic solvent. The corresponding zeta potentials measured in NMP do not exceed 5 mV, i.e., the particles are almost neutral and a noticeable aggregation takes place. This fact evidences that the usual particle size information found in literature referred to water is valuable, but differs of the actual membrane manufacture conditions.

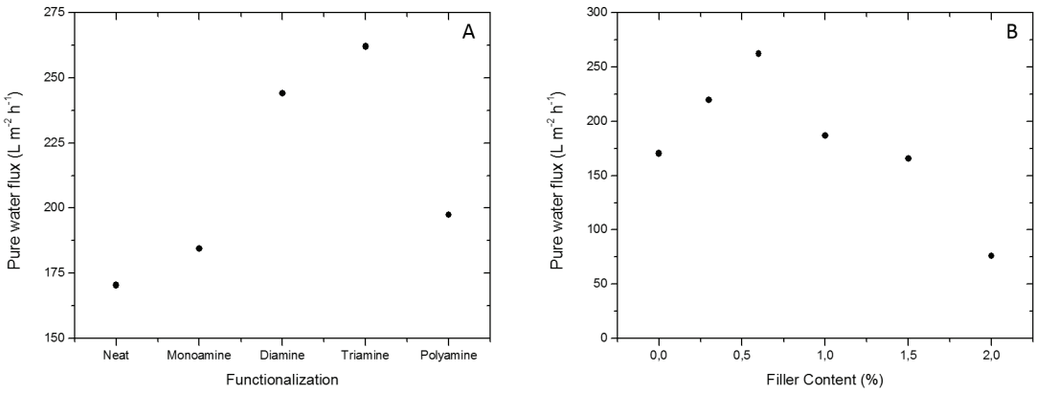

Fig. 6. Membrane pure water flux experiments: (A) Influence of organic functionalization of fillers; (B) Influence or particle concentration for SBA-15/triamine.

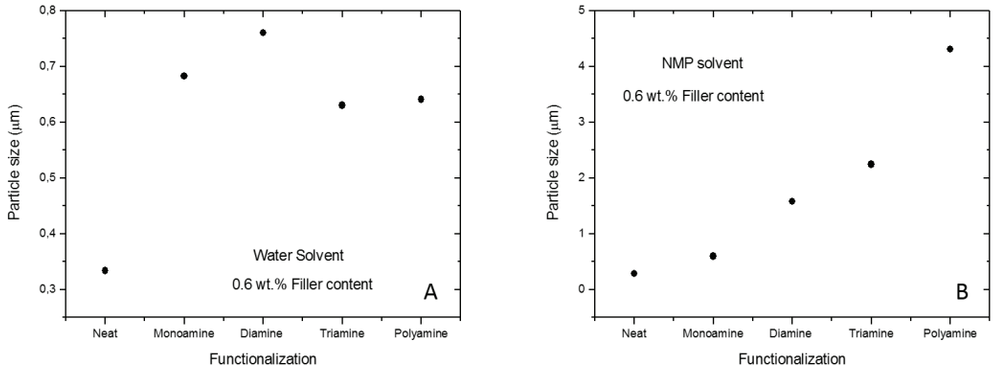

Fig. 7. Influence of functionalization type on the average size of particles used as fillers. (A) Average particle size in water. (B) Average particle size in NMP.

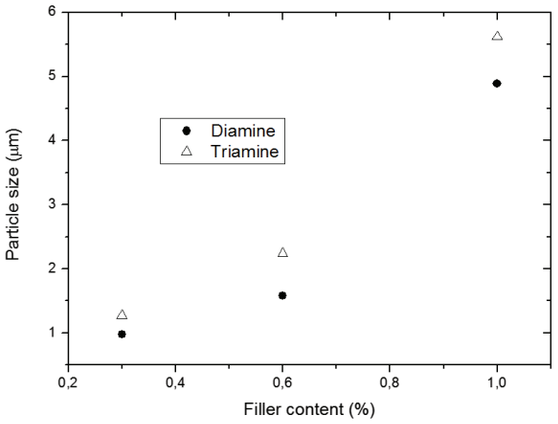

Fig. 8. Effect of filler concentration in NMP on the average particle size.

Additional experiments have been carried out to check the effect of filler content on particle size. The results are displayed in Fig. 8 for SBA-15/Diamine and SBA-15/Triamine systems dispersed in NMP. As expected, the aggregation of particles is promoted in both cases, probably due to reinforced van der Waals interaction, when filler concentration increases.

By comparing Figs. 6–8, no simple correlation between membrane water permeation and particle size can be found; although it seems that there exist a defined particle dimension that limits the membrane performance. Two alternative routes, changing the filler concentration or chemically modifying the filler surface, can achieve the highest water flux.

3.5. Influence of membrane porosity

3.5.1. Overall and surface porosity

In the Introduction Section, three different methodologies to characterize the porosity of membranes were discussed. In order to estimate the surface pores porosity [Eq. (1)] and density of surface pores [Eq. (2)] of prepared membranes, surface images have been taken by FEG-SEM (Fig. 2). Likewise, overall porosity calculated by Eq. (3) has been determined from water uptake experiments.

Fig. 9 shows a comparison of porosity values calculated by these different procedures to evaluate the porosity effect on the membrane permeation performance for 0.6 wt.% filler content. The correlation between porosity and filler functionalization obtained from water-uptake experiments (Fig. 9(A)) is quite different to those found by direct measure of surface pores number estimated from FEG-SEM images (Figs. 9(B) and (C)). It is evident that the excellent agreement between membrane permeation (Fig. 6A) and surface porosity parameters (Figs. 9(B) and (C)) is lost when overall porosity is considered (Fig. 9(A)). As mentioned in the Introduction Section, the overall porosity calculated by water sorption capacity is only valid for symmetrical structures and just yields valuable information about the free volume of materials. Taking into account that porosity of membrane surface largely determines the water permeation is fair to consider preferentially the contribution of surface porosity parameters to the morphological analysis of membranes.

The rather slight differences observed between Figs. 9(B) and (C) could be related to the topology of surface pores. If all formed pores were identical in size and geometry, both porosity parameters should exhibit the same trend. Therefore, the next Section is devoted to a more detailed analysis of membrane surface porosity.

3.5.2. Average pore size and shape

Fig. 10 illustrates the influence of filler amine-functionalization on the average pore size of membranes prepared in this investigation. A fair correlation is observed between this parameter calculated by statistical analysis of FEG-SEM images (Fig. 10(A)) and the water permeation (Fig. 6A)). Therefore, the permeation improve due to filler modification can be caused by two cooperative effects, the increment of the surface pores number and their average size. Both facts contribute significantly to increase the membrane permeation.

For comparison purpose, functional pore size estimated from MWCO values is shown in Fig. 10(B). It seems apparent that the MWCO parameter is a valuable tool to estimate the rejection potential of membranes; however,

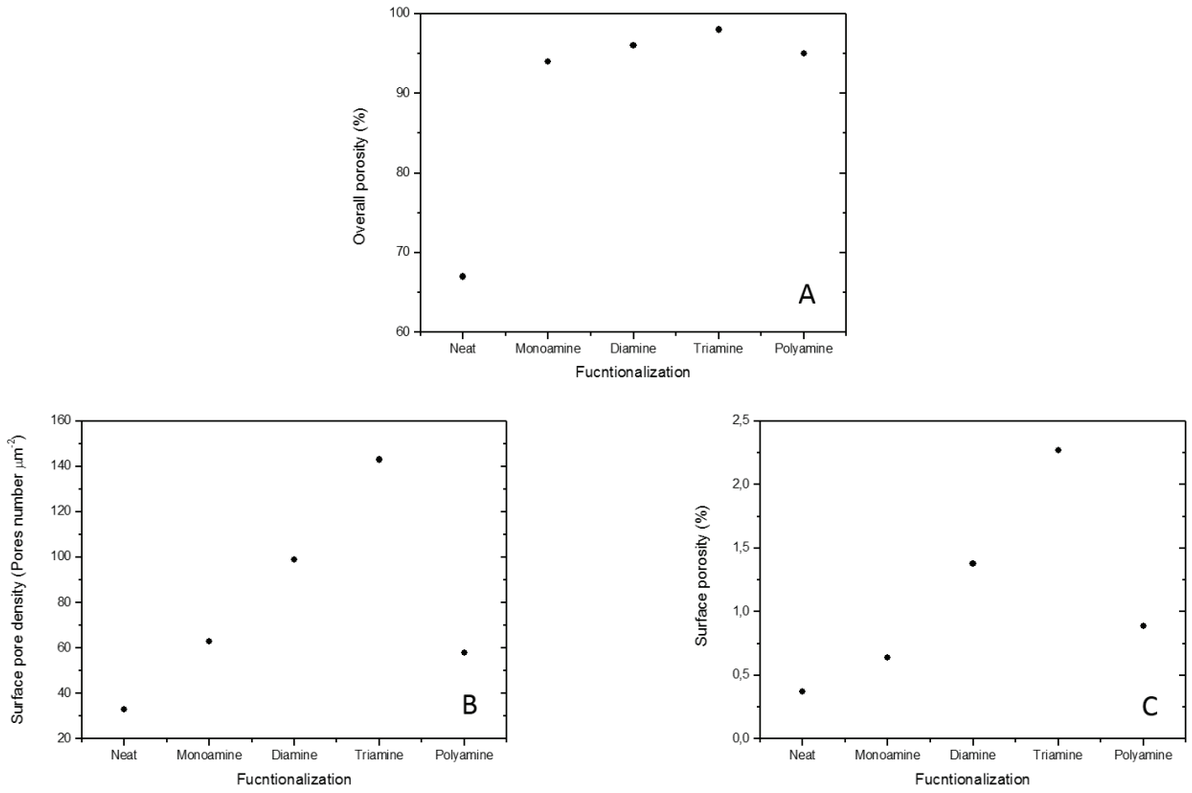

Fig. 9. Porosity analysis of prepared membranes as function of particle functionalization at 0.6 wt. % filler content. (A) Overall porosity; (B) Surface pores density; (C) Surface porosity.

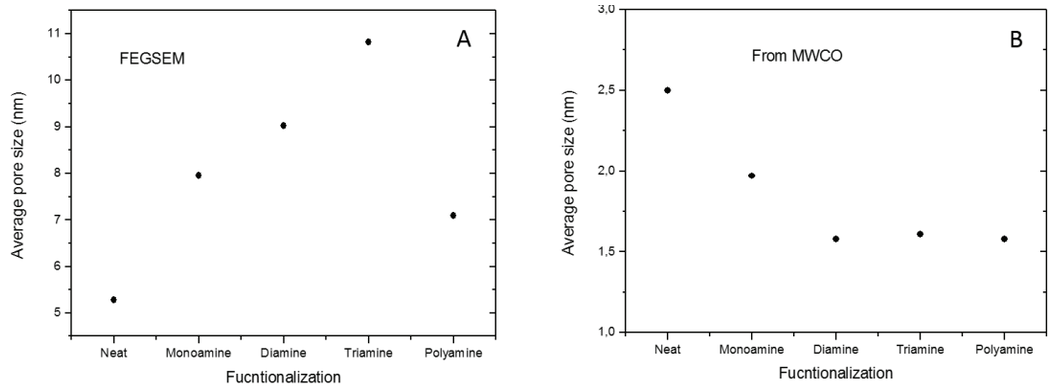

Fig. 10. Influence of particle functionalization on the estimated average pore size of membranes: (A) Physical average pore size determined by direct measure; (B) Functional dimensions of pores estimated from rejection experiments.

Fig. 10(B) clearly shows that is not possible to predict the membrane water permeation taking into account exclusively the observed membrane rejection for a specific model solute.

In order to clarify the effect of pore topology on the membrane permeation performance, the circularity of pores (geometrical roundness) was calculated by statistical analysis of membrane pores geometry.

Figs. 11(A) and (B) show the pore circularity distribution for samples corresponding to Neat and Triamine membranes. The calculated average pore circularity of prepared membranes in this study is displayed in Fig. 11(C). It is evident that the amount of non-circular pores increases with amine functionalization that promotes the formation of pores with irregular shapes. The presence of fillers with dissimilar sizes, shapes, and textural properties disrupts the polymer chains in different forms and produces a variety of pore geometries. Therefore, a complete porosity analysis of surface membrane should consider the pore topology.

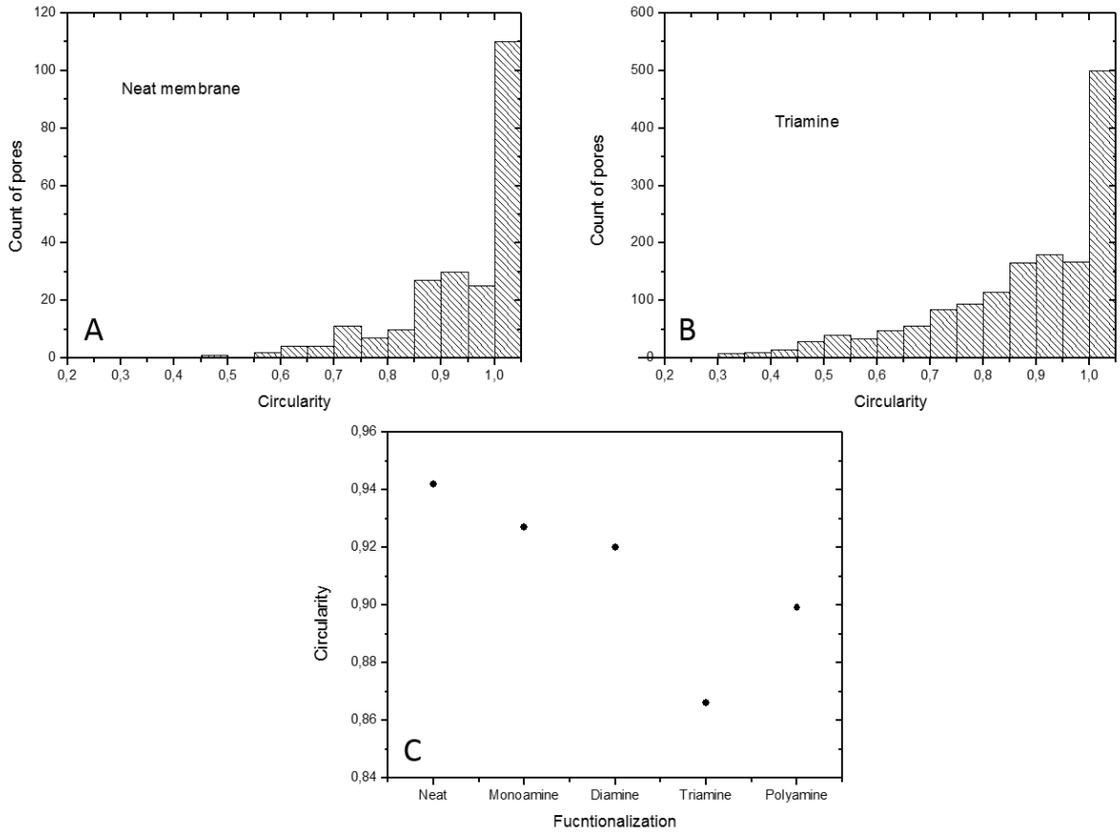

Fig. 11. Statistical analysis of surface pores geometry of prepared membranes: (A) Pore circularity distribution of neat PES membrane; (B) Pore circularity distribution of triamine membrane; (C) Calculated average values of circularity for membranes used in this study.

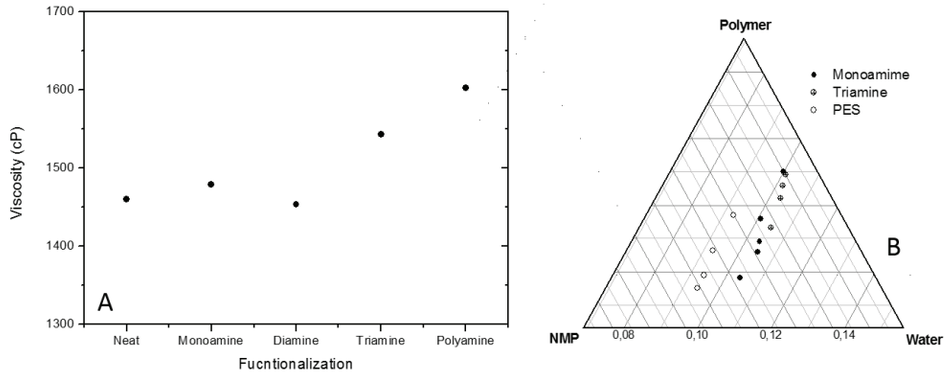

Fig. 12. Kinetics and thermodynamics features of membrane formation process: (A) Viscosity of casting polymeric solution used for membrane preparation; (B) Effect of amine functionalization on cloud point curves of casting solutions.

3.6. Kinetics and thermodynamics of membrane formation process

To explore the causes that explain the observed morphological characteristics of prepared membranes, the phase inversion process was investigated through the analysis of some kinetic and thermodynamic features involved on the membrane formation (Fig. 12).

The viscosity of the casting solution mainly alters the exchanging rate of solvent and non-solvent during phase inversion due to its hindrance effect on the fluids transport. Fig. 12(A) shows that the viscosity of casting solutions was rather similar for all tested systems. Thus, the analysis of this variable cannot explain in detail the observed morphological changes between neat and doped membranes. Perhaps, the observed reduction of permeation for polyamine membrane (Fig. 6(A)) could be associated to the more viscous cast system that would promote the thicker skin layer formation [28].

On the other hand, the ternary diagram of polymer, solvent, non-solvent system is shown in Fig. 12(B) to compare the thermodynamic stability through the cloud point curves. The modified membranes need higher non-solvent percentages for the precipitation to occur. In other words, the water tolerance of doped membranes is increased as result of filler incorporation into the polymeric solution. Therefore, as the bimodal line moves along the solvent-non solvent axis, more porous morphology is obtained. As result of filler incorporation, the demixing rate of solvent-nonsolvent is increased promoting the formation of pores. The effect of particle functionalization extent in terms of number of amino groups incorporated to the surface of SBA-15 is not remarkable and both mono and triamine modifications show similar water tolerance values.

A similar observation has been recently published by Garcia-Ivars et al. using nanoparticles with different hydrophilic character [36]. These authors suggest that the observed similarity in water tolerance should be explained in terms of morphological effects due to thermodynamic shifts rather than filler hydrophilicity. Then, the specific functionalization used would be irrelevant.

3.7. Effect of membrane hydrophilicity

Contact angle between water and surface of doped membranes was measured and compared with the neat membrane (Fig. 13) that resulted the most hydrophobic material. A fair decreasing trend in contact angle was found as the particle amine-functionalization extent enlarged.

It is usually accepted that the increase of membrane hydrophilicity should enhance the water permeation; but in this case, there is no total correlation between these two membrane properties. The most hydrophilic material, Polyamine, did not result in the better membrane permeation. However, the improved hydrophilic surface of membrane could play an important role in the desired increase of fouling resistance against organic foulants.

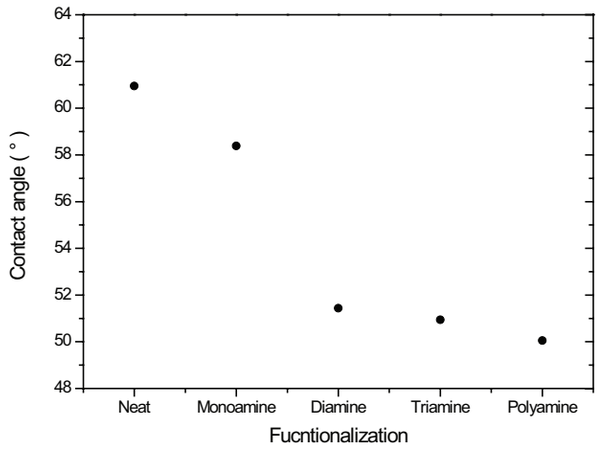

Fig. 13. Contact angle of neat and modified membranes.

4. Conclusions

- Successful functionalization with amino groups of filler proposed in this investigation, SBA-15, was confirmed by textural properties study and elemental analysis.
- The growing amine-functionalization of fillers by co-condensation method promotes an increase of water membrane permeation. The effect of hyperbraching synthesis procedure was less pronounced on the membrane performance.
- Particle size of doping fillers dispersed in the polymer solvent, namely NMP, increased as result of SBA-15 amine-functionalization. Conversely, particle size of functionalized fillers was hardly affected in water. Aggregation in NMP significantly produces higher particle sizes as compared with water.
- A good agreement was found between surface membrane porosity and water permeation. The effect of pore shape, described in circularity terms, should be considered for a rigorous analysis of porosity effect on the membrane performance.
- Through the thermodynamics of membrane formation process was possible to clarify the effect of particle amine-functionalization on the morphology of prepared membranes.
- The hydrophilic character of membrane surface was enhanced according to rising amine-functionalization of incorporated particles. However, the most hydrophilic material (Polyamine) did not show the highest water flux.

Acknowledgements

The Regional Government of Madrid through program S2013/MAE-2716-REMTAVARES-CM which is co-financed with structural founding of European Community (REMTAVARES, S2013/MAE-2716) is acknowledged for the financial support of this research. Likewise, the authors gratefully thank the financial support of the Spanish government (CTQ2011-22707, CTQ2014-57858-R programs). Thanks are also given to Genesys Membrane Product, S.L. for its valuable contribution to this work.

References

[1] J. Kim, B. Van der Bruggen, The use of nanoparticles in polymeric and ceramic membrane structure: review of manufacturing procedures and performance improvement for water treatment, Environ. Pollut., 158 (2010) 2335–2349.
[2] L. Y. Ng, A. W. Mohammad, C. P. Leo, N. Hilal, Polymeric membranes incorporated with metal/metal oxide nanoparticles: a comprehensive review, Desalination, 308 (2013) 15–33.
[3] G. L. Jadav, P. S. Singh, Synthesis of novel silica-polyamide nanocomposite membrane with enhanced properties, J. Membr. Sci., 328 (2009) 257–267.
[4] A. Bottino, G. Capannelli, V. D'Asti, P. Piaggio, Preparation and properties of novel organic–inorganic porous membranes, Sep. Purif. Technol., 22–23 (2001) 269–275.
[5] K. Ebert, D. Fritsch, J. Koll, C. Tjahjawiguna, Influence of inorganic fillers on the compaction behavior of porous polymer based membranes, J. Membr. Sci., 233 (2004) 71–78.
[6] A. Sotto, A. Boromand, S. Balta, J. Kim, B. Van der Bruggen, Doping of polyethersulfone nanofiltration membranes: antifouling effect observed at ultralow concentrations of TiO_2, J. Mat. Chem., 21 (2011) 10311–10320.

[7] J. Dolina, T. Jırıcek, T. Lederer, Biocide modification of ultrafiltration membranes using nanofiber structures, Desal. Wat. Treat., 56 (2015) 3252–3258.
[8] L. Liu, M. Son, S. Chakraborty, C. Bhattacharjee, H. Choi, Fabrication of ultra-thin polyelectrolyte/carbon nanotube membrane by spray-assisted layer-by-layer technique: characterization and its anti-protein fouling properties for water treatment, Desal. Wat. Treat., 51 (2013) 6194–6200.
[9] J. Yin, B. Deng, Polymer-matrix nanocomposite membranes for water treatment, J. Membr. Sci., 479 (2015) 256–275.
[10] A. Sotto, A. Boromand, S. Balta, S. Darvishmanash, J. Kim, B.Van der Bruggen, Nanofiltration membranes enhanced with TiO_2 nanoparticles: a comprehensive study, Desal. Wat. Treat., 34 (2011) 179–183.
[11] Y. Yang, H. Zhang, P. Wang, Q. Zheng, J. Li, The influence of nano-sized TiO_2 fillers on the morphologies and properties of PSF UF membrane, J. Membr. Sci., 288 (2007) 231–238.
[12] L. Y. Yu, H. M. Shen, Z.L. Xu, PVDF-TiO_2 composite hollow fiber ultrafiltration membranes prepared by TiO_2 sol–gel method and blending method, J. Appl. Polym. Sci., 113 (2009) 1763–1772.
[13] N. Maximous, G. Nakhla, W. Wan, K. Wong, Effect of the metal oxide particle distributions on modified PES membranes characteristics and performance, J. Membr. Sci., 361 (2010) 213–222.
[14] J. Li, Z. Xu, H. Yang, L. Yu, M. Liu, Effect of TiO_2 nanoparticles on the surface morphology and performance of microporous PES membrane, Appl. Surf. Sci., 255 (2009) 4725–4732.
[15] A. Razmjou, J. Mansouri, V. Chen, The effects of mechanical and chemical modification of TiO_2 nanoparticles on the surface chemistry, structure and fouling performance of PES ultrafiltration membranes, J. Membr. Sci., 378 (2011) 73–84.
[16] X. Cao, J. Ma, , X. Shi, Z. Ren, Effect of TiO_2 nanoparticle size on the performance of PVDF membrane, Appl. Surf. Sci., 253 (2006) 2003–2010.
[17] C. Liao, J. Zhao, P Yu, H Tong, Y. Luo, Synthesis and characterization of low content of different SiO_2 materials composite poly (vinylidene fluoride) ultrafiltration membranes, Desalination, 285 (2012) 117–122.
[18] L.D. Nghiem, A.I. Schäfer, M. Elimelech, Removal of natural hormones by nanofiltration membranes: measurement, modeling, and mechanisms, Environ. Sci. Technol., 38 (2004) 1888–1896.
[19] M.J. López-Muñoz, A. Sotto, J.M. Arsuaga, B. Van der Bruggen, Influence of membrane, solute and solution properties on the retention of phenolic compounds in aqueous solution by nanofiltration membranes, Sep. Purif. Technol., 66 (2009) 194–201.
[20] M. Ulbricht, Advanced functional polymer membranes, Polymer, 47 (2006) 2217–2262.
[21] L. Yan, Y. S. Li, C.B. Xiang, S. Xianda, Effect of nano-sized Al_2O_3-particle addition on PVDF ultrafiltration membrane performance, J. Membr. Sci., 276 (2006) 162–167.
[22] H. Danxi, W. Lei, M. Xiaorong, W.Xudong, B. Juanli, Study on the effect of modified PVDF ultrafiltration membrane for secondary effluent of urban sewage, Desal. Wat. Treat., 52 (2014) 5084–5091.
[23] A. Razmjou, A. Resosudarmo, R.L. Holmes, H. Li, J. Mansouri, V.Chen, The effect of modified TiO_2 nanoparticles on the polyethersulfone ultrafiltration hollow fiber membranes, Desalination, 287 (2012) 271–280.
[24] M. Peyravi, M. Jahanshahi, A. Rahimpour, A. Javadi, S. Hajavi, Novel thin film nanocomposite membranes incorporated with functionalized TiO_2 nanoparticles for organic solvent nanofiltration, Chem. Eng. J., 241 (2014) 155–166.
[25] H.M. Schaink, J.A.M. Smit, Toward an integrated analytic description of demixing in ternary solutions of non ideal uncharged lattice polymers, hard particles, and solvent, Macromolecules, 29 (1996) 1711–1720.
[26] A.J. Reuvers, J.W.A. van den Berg, C.A. Smolders, Formation of membranes by means of immersion precipitation: Part I. A model to describe mass transfer during immersion precipitation, J. Membr. Sci., 34 (1987) 45–65.
[27] P. van de Witte, P.J. Dijkstra, J.W.A. van den Berg, J. Feijen, Phase separation processes in polymer solutions in relation to membrane formation, J. Membr. Sci., 117(1996) 1–31.
[28] P. Aerts, I. Genne, S. Kuypers, R. Leysen, I.F.J Vankelecom, P.A Jacobs, Polysulfone–aerosil composite membranes: Part 2. The influence of the addition of aerosil on the skin characteristics and membrane properties, J. Membr. Sci., 178 (2000) 1–11.
[29] Y. Yang, W. Jun, Z. Qing-zhu, C. Xue-si, Z. Hui-xuan, The research of rheology and thermodynamics of organic–inorganic hybrid membrane during the membrane formation, J. Membr. Sci., 311 (2008) 200–207.
[30] D. Zhao, J. Feng, Q. Huo, N. Melosh, G.H. Fredrikson, B.F. Chmelka, G.D. Stucky, Triblock copolymer syntheses of mesoporous silica with periodic 50 to 300 angstrom pores, Science, 279 (1998) 548–552.
[31] F. Hoffmann, M. Cornelius, J. Morell, M. Fröba, Silica-based mesoporous organic-inorganic hybrid materials, Angew. Chem. Int., 45 (2006) 3216–3251.
[32] A. Martín, R.A. García, D. Sen Karaman, J.M. Rosenholm Polyethyleneimine-functionalized large pore ordered silica materials for poorly water-soluble drug delivery, J. Mater. Sci., 49 (2014) 1437–1447.
[33] A. Sotto, A. Boromand, R.X. Zhang, P. Luis, J.M. Arsuaga, J. Kim, B. Van der Bruggen, Effect of nanoparticle aggregation at low concentrations of TiO_2 on the hydrophilicity, morphology, and fouling resistance of PES–TiO_2 membranes, J. Colloid Interface Sci., 363 (2011) 540–550.
[34] X. Zhang, B. Shi, X. Liu, Preparation of polysulfone ultrafiltration membranes modified by silver particles, Desal. Wat. Treat., 51 (2013) 3762–3767.
[35] C.Y. Lai, A. Groth, S. Gray, M. Duke, Investigation of the dispersion of nanoclays into PVDF for enhancement of physical membrane properties, Desal. Wat. Treat., 34 (2011) 251–256.
[36] J. Garcia-Ivars, M.-I. Iborra-Clar, M.-I- Alcaina-Miranda, B. Van der Bruggen, Comparison between hydrophilic and hydrophobic metal nanoparticles on the phase separation phenomena during formation of asymmetric polyethersulphone membranes, J. Membr. Sci., 493 (2015) 709–722.